Supplement of Atmos. Chem. Phys., 16, 6381–6393, 2016
http://www.atmos-chem-phys.net/16/6381/2016/
doi:10.5194/acp-16-6381-2016-supplement
© Author(s) 2016. CC Attribution 3.0 License.

Atmospheric Chemistry and Physics Open Access EGU

Supplement of

Bidirectional air–sea exchange and accumulation of POPs (PAHs, PCBs, OCPs and PBDEs) in the nocturnal marine boundary layer

Gerhard Lammel et al.

Correspondence to: Gerhard Lammel (lammel@recetox.muni.cz)

The copyright of individual parts of the supplement might differ from the CC-BY 3.0 licence.

Contents

S1 Methodology

S1.1 Substance properties

For the fugacity ratio calculation based on the Whitman two-film model (Bidleman and McConnell, 1995), the Henry's law constant was corrected for the sea water temperature and the salt water (by the Setschenow constant, e.g., Zhong et al., 2012).

Table S1. References of physico-chemical properties used. H = Henry's law constant, dU_{aw} = enthalpy of water-air phase change, K_S = salting-out (Setschenow) constant. Substances addressed: see main text.

	PAHs	PCBs	OCPs	PBDEs
H	Bamford et al., 1999	Li et al., 2003	Cetin et al., 2006	Cetin and Odabasi, 2005; Tittlemier et al., 2002
dU_{aw}	Bamford et al., 1999	Li et al., 2003	Cetin et al., 2006	Cetin and Odabasi, 2005
K_S	Jonker and Muijs, 2010 [(a)]	Rowe et al., 2007	Lohmann et al., 2012; Cetin et al., 2006	Jonker and Muijs, 2010 [(b)]

[(a)] assumed to be given by value for isomer in case of lack of data
[(b)] adopted estimate

S1.2 Analytical quality assurance parameters

Table S2: Instrument limits of quantification (ILOQ) for various types of sample, given as masses and concentrations

Analyte	Mass	concentration	
	(pg)	air (pg m^{-3})	water (pg L^{-1})
PAHs	160-840	6-34	0.5-4.2
PCBs and OCPs	50-510	7-23	0.05 - 0.5
PBDEs	0.083-0.953	0.003-0.304	0.0003 - 0.037

S1.3 Vertical flux calculations by micrometeorological techniques

Two micrometeorological methods, the aerodynamic and the eddy covariance technique, have been applied to derive turbulent vertical gaseous organics fluxes (F_c, in ng m^{-2} s^{-1}). According to the aerodynamic method (Hicks et al., 1987; Kuhn et al., 2007), F_c is the product of the vertical difference of gaseous organics concentration, Δc_z (ng m^{-3}), and the turbulent transfer velocity, v_{tr} (m s^{-1}):

$$F_c = - v_{tr} \Delta c_z = - v_{tr} [c(z_2) - c(z_1)] \quad \text{(S1)}$$

where z_2 and z_1 are the heights of inlets of gaseous organics' sampling (1.05 m and 2.80 m, see section 2.1). The transfer velocity, a measure of the vertical turbulent (eddy) diffusivity between z_2 and z_1, is simply the inverse of the aerodynamic resistance, R_a (s m^{-1}), against the vertical transport:

$$R_a = v_{tr}^{-1} = (\kappa u_*)^{-1} [\ln(z_{r,2} / z_{r,1}) - \Psi_H(z_{r,2} / L) + \Psi_H(z_{r,1} / L)] \quad \text{(S2)}$$

where κ is the von Karman constant (= 0.4), u_* is the friction velocity (in m s^{-1}), $z_{r,i} = z_i - d$ is the relative height (in m), and d = 0.34 m is the zero-plane displacement height for the Selles Beach site, derived by the eddy covariance technique. Applying the Monin-Obukhov similarity theory (Monin and Obukhov, 1954) for the mathematical description of turbulent transport in the atmospheric surface layer, a characteristic length scale, the Obukhov length L (in m; Obukhov, 1948) is the quantitative measure of the relation between dynamic (friction) and thermal (buoyancy) forces which drive the turbulent transport,

$$L = - u_*^3 \, [\kappa \; g \, T_{air}^{-1} \; H \, (c_p \rho_{air})^{-1}]^{-1} \quad \text{(S3)}$$

where T_{air} is the air temperature (K), c_p is the specific heat of air at constant pressure (1004.7 $m^2 s^{-2} K^{-1}$), g the acceleration of gravity (9.807 m s^{-2}), and H the turbulent sensitive heat flux (W m^{-2}). When applying the eddy covariance technique, the key micrometeorological quantities u_* and H were derived from fast response (20 Hz) measurements of the three spatial components of the 3D wind vector and the air temperature. For control of the atmospheric surface layer's thermodynamic stratification vertical gradients of wind speed (u) and air temperature (T_{air}) have been used which in turn have been derived from continuous measurements of wind speed and air temperature at four levels (0.34, 0.70, 1.45, and 3.00 m above ground) at Selles Beach. The dimensionless integrated similarity functions (or integrated stability correction functions) $\Psi_H(z_{r,2}/L)$ and $\Psi_H(z_{r,1}/L)$ for heat were calculated after Paulson (1970).

S1.4 Non-steady state two-box model

A non-steady state 2-box model was applied to test the hypothesis that the diurnal variation of POP concentrations in air during 6-10 July is explained by local processes, namely the combination of volatilisation from the sea surface and atmospheric mixing depth.

The model simulations for the period 6-10 July 2012 were initialised by observed surface seawater concentrations, c_w (Table 2), and modelled marine boundary layer depths (Lagrangian dispersion model; see Section 2.2). Temperature and wind speed data were taken from measurements at the site (Cretan north coast). Winds were on-shore throughout the simulated period. Input data are listed in Table S3. Gaseous air and seawater concentrations and the air-sea exchange flux, F_{aw}, are output.

Substances for which input data were incomplete or insufficient observational data were available (model evaluation) were not simulated. Upon input, simultaneous measurements of air and seawater concentrations are lacking for HCH and 3-ring PAHs (see Section 2.5) and some physic-chemical properties are lacking for PeCB. Insufficient air concentration and flux measurements during 6-10 July are available for DDE. Input parameters for the 2-box model are listed in Table S3. The biogeochemical parameters had been used earlier to simulate the air-sea exchange of a PAH in the same region (Mulder et al., 2014).

Table S3. Input parameters for the 2-box model, (a.) environmental, (b.) substance specific.

a.

Parameter	Unit	Value adopted or mean (min-max)	Reference
OH concentration in air	molec cm^{-3}	1.5×10^{6} during day-time, 0 during nighttime	climatological data (Spivakovsky et al., 2000)
Dissolved organic carbon concentration in seawater	µM	61.5	Pujo-Pay et al., 2011
Atmospheric mixing height	m	522 (131-1295)	Modelled (see section 2.2, Fig. S1)
Mixing depth in ocean	m	40	d'Ortenzio et al., 2005
Concentration of particulate organic carbon in surface seawater	µM	3.08	Pujo-Pay et al., 2011
Air temperature	K	302.1 (299.1 – 305.1)	Measured
Surface seawater temperature (SST)	K	297.4 (297.0 – 297.9)	satellite-retrieved data [a]
Export (settling) velocity of particle-sorbed molecule in seawater	m s^{-1}	8×10^{-7}	Schwarzenbach et al., 2003, divided by a factor of 10 (Mulder et al., 2014, upper estimate parameter set)
Deposition velocity of particle-sorbed molecule in air	m s^{-1}	6.5×10^{-5}	Franklin et al., 2000

[a] AVHRR (Advanced Very High Resolution Radiometer), 1.5 × 1.5 km resolution; source: eoweb.dlr.de:8080

b.

Parameter	Unit	Value adopted or mean (min-max)	Reference
Henry coefficient	Pa m^{-3} mol^{-1}	FLT/PYR: 1.96/1.71 PCB28/PCB52: 18.1/14.8 PBDE47/PBDE99: 0.85/0.60	Bamford et al., 1999; Li et al., 2003; Cetin and Odabasi, 2005
1st order degradation rate coefficient in seawater	10^{-9} s^{-1}	FLT/PYR: 4.2/2.8 PCB28/PCB52: 2.2/1.2 PBDE47/PBDE99: 0/0	Value for freshwater (USEPA, 2009) divided by 10; Value for water (Beyer et al., 2000; Wania and Daly, 2002) divided by 10; T dependence: EU, 1996; assumed to be 0 in lack of data
Gas-phase reaction rate coefficient with OH	10^{-12} cm^3 $molec^{-1}$ s^{-1}	FLT/PYR: 11/50 PCB28/PCB52: 0.934/0.0162 PBDE47/PBDE99: 1.5/0.80	Keyte et al., 2013; Anderson and Hites, 1996; USEPA, 2009; Raff and Hites, 2007
Octanol/water partitioning coefficient K_{ow}	log	FLT/PYR: 5.16/4.88 PCB28/PCB52: 5.66/5.91 PBDE47/PBDE99: 6.11/6.61	Calvert et al., 2002; Li et al., 2003; Hayward et al., 2006
Dissolved organic carbon/water partition coefficient	L g^{-1}	0.411× K_{ow}	Karickhoff, 1981
Particulate organic carbon/water partitioning coefficient	L g^{-1}	K_{ow}	assumed to be given by K_{ow} (Rowe et al., 2009)
Setschenow constant	L mol^{-1}	FLT/PYR: 0.364/0.354 PCB28/PCB52: 0.3/0.3 PBDE47/PBDE99: 0.35/0.35	Jonker and Muijs, 2010; Cetin et al., 2006; Rowe et al., 2007; Jonker and Muijs, 2010
Particulate mass fraction in air		0.05 (0.02 - 0.14)	Measured

Table S4. Measured sea surface temperature 6-10 July 2012 (°C), AVHRR, 12 h means, resolution 1.5 × 1.5 km (Valavanis et al., 2004), input for simulation of c_a

Date	Day	Night
20120706	24.749	23.837
20120707	24.202	23.972
20120708	24.626	24.536
20120709	24.115	24.297
20120710	23.91	23.914

Fig. S.1. Modelled atmospheric mixing depth (m) 6-10 July 2012 (UTC), input for simulation of c_a

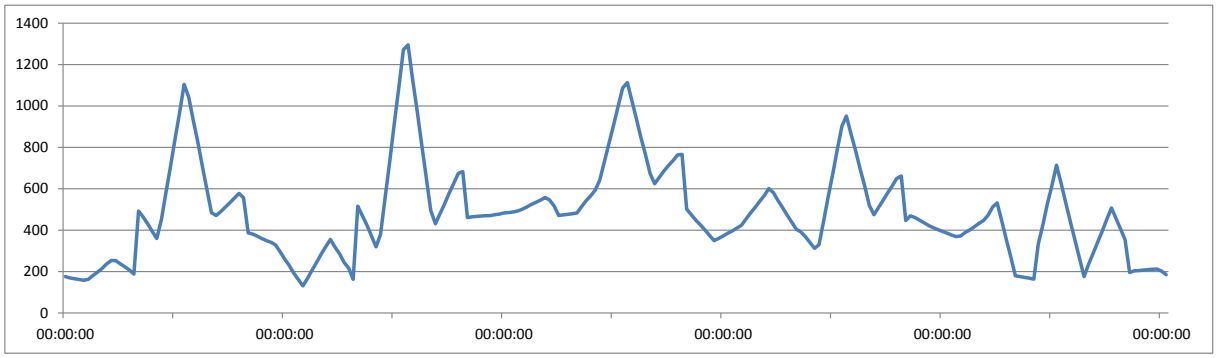

S2 Results

S2.1 Meteorological situation

During 2-11 July 2012 the Aegean was mostly influenced by northerly, and in its northern part easterly advection over the Marmara Sea as part of a cyclonic system which resided over Romania during 1-3 July and over western Russia during 4-10 July. The sky was cloud-free all the time. No frontal passage occurred, such that for all samples taken in the study region the hypothesis of horizontal homogeneity of air mass collected can be applied. Under the influence of a strong westerly flow towards Europe the flow in the northern part of the Aegean switched to westerly during the night 11-12 July, such that air which was residing over the SW Balkans was advected as well as air from beyond, i.e. central Italy and the NW Mediterranean Sea and the Iberian Peninsula.

The local meteorological situation for the entire sampling campaign (2–13 July 2012) is given in Fig. S2, showing the temporal course of wind speed and direction measured at the position of one of the automatic weather stations at Selles Beach. Surprisingly, >80% of the campaign (and >95% of the gradient measurements i.e., horizontal bars in Fig. S2) experienced wind speeds > 4 m s^{-1}. Under such conditions a local wind system (land-sea breeze) is most unlikely. Consequently, as soon as the wind speed breaked down to < 3 m s^{-1}, land-sea breeze occurred (nights 5-6 July, 13-14 July, Fig. S2) Under these conditions the atmospheric

surface layer is usually very well mixed due to the dynamic forces (friction), such that thermal stability corrections in eq. (S2) can be neglected ($\Psi_H(z_{r,2}/L) = \Psi_H(z_{r,1}/L) \approx 0$).

The local wind direction, however, was almost thoroughly from the west (270°), within a quite narrow range (259°–300°; averages during individual sampling periods given in Fig. S2). Only winds between 270° and 40° (condition for onshore winds) could be considered for the evaluation of turbulent vertical fluxes, F_c, from and to seawater. All individual sampling periods with more than 10% of the time outside this wind sector were rejected (nights 3-4 July, 4-5 July, 6-7 July, 7-8 July, 8-9 July, 9-10 July, 10-11 July).

Fig. S2: Wind speed (magenta) and wind direction (grey) observed on Selles Beach during 2-14 July 2012. White circles represent central values of sampling intervals. Horizontal bars indicate the length of intervals. Green shaded area = on-shore winds. For flux calculations only intervals with on-shore wind were used.

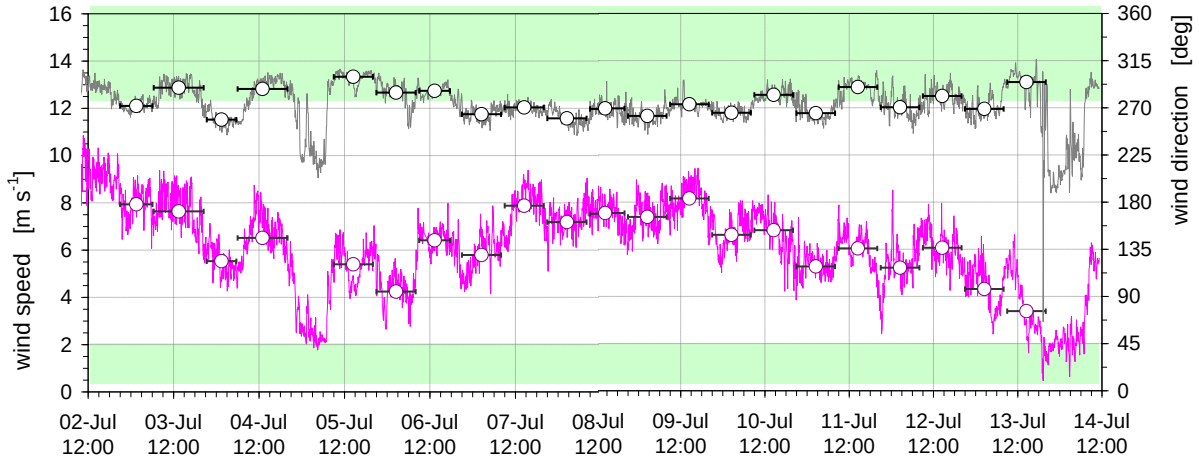

S2.2 Transfer velocity

The time series of turbulent transfer velocity, v_{tr}, at Selles Beach, derived from micrometeorological measurements by eddy covariance technique (sections 2.4, S1.3), is shown in Fig. S3. Data represent temporal averages of 30 min v_{tr} values over each individual sampling period (mostly 11 h), horizontal bars indicate the length of the sampling period, and vertical error bars correspond to ± 1σ of the respective v_{tr} mean. Since only those data from periods with

winds from the sea (onshore winds between 270° and 40°) could be considered for suitable fetch conditions, data of the nights 3-4 July and in the period 6-11 July have not been used for calculations of vertical fluxes. Values of transfer velocity range between approx. 2.5 and 7.5 cm s^{-1}, and – since turbulent transport at Selles Beach was dominated by dynamic forces, v_{tr} data mirror more or less those of horizontal wind speed (see Fig. S2).

Fig. S3: Turbulent transfer velocities (cm s^{-1}) during the field campaign at Selles Beach, Crete (35.2°N, 24.4°E) during 2-13 July 2012. Eddy covariance technique and calculations have been applied to derive these data from measurements of fast response (20 Hz) measurements of key micrometeorological parameters (details, see S1.3).

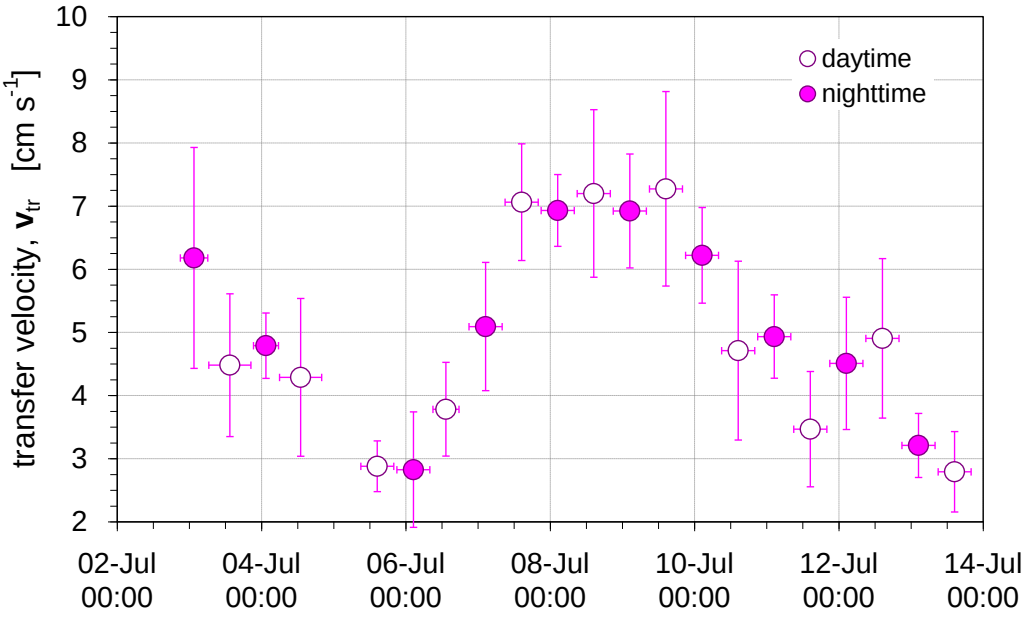

S2.3 Atmospheric concentration and flux data

Table S3. Concentrations at ground level, z_1 = 1.05 m, of (a.) gaseous and particulate PAHs (ng m^{-3}), and (b.) gaseous OCPs (ng m^{-3}), PCBs (ng m^{-3}) and gaseous and particulate PBDEs (pg m^{-3}) from 3 July 2012 day-time (D) until 13 July 2012 day-time. N = night-time. Upper limits: Insignificant data (<3 standard deviations of field blank concentrations). Data from 6 July D until 10 July D based on 2 replica measurements (mean).

a.

	ACE		PHE		FLT		PYR	
	g	p	g	p	g	p	g	p
3 July D	<0.058	<0.004	2.933	0.159	0.893	0.117	0.367	<0.003
3-4 July N	<0.096	<0.004	1.058	0.294	0.759	0.198	0.344	<0.003
4 July D	<0.058	<0.004	3.543	0.158	0.782	0.162	0.858	<0.003
4-5 July N	n.d.	n.d.	n.d.	n.d.	n.d.	n.d.	n.d.	n.d.
5 July D	<0.072	<0.004	2.366	0.126	0.634	<0.019	0.237	<0.003
5-6 July N	0.274	n.d.	4.507	n.d.	0.828	n.d.	0.930	n.d.
6 July D	0.068	<0.004	1.363	0.672	0.549	0.354	0.276	0.111
6-7 July N	0.119	<0.004	1.375	0.374	0.301	0.208	0.152	0.064
7 July D	0.081	<0.004	1.047	0.290	0.248	0.152	0.140	0.056
7-8 July N	0.116	<0.004	1.339	0.309	0.265	0.159	0.149	0.065
8 July D	0.091	<0.004	1.693	0.260	0.261	0.152	0.145	0.056
8-9 July N	0.107	<0.004	2.339	0.234	0.271	0.134	0.132	<0.003
9 July D	0.081	n.d.	0.591	n.d.	0.239	n.d.	0.090	n.d.
9-10 July N	0.110	<0.004	1.864	0.266	0.289	0.144	0.136	0.060
10 July D	0.059	<0.004	1.256	0.200	0.263	0.124	0.130	<0.003
10-11 July N	0.083	n.d.	0.756	n.d.	0.264	n.d.	0.133	n.d.
11 July D	n.d.	n.d.	n.d.	n.d.	n.d.	n.d.	n.d.	n.d.
11-12 July N	<0.072	<0.004	0.308	<0.065	0.046	<0.019	<0.10	<0.003
12 July D	<0.072	<0.004	0.246	<0.065	0.044	<0.019	<0.10	<0.003
12-13 July N	<0.072	<0.004	0.215	<0.065	0.059	<0.019	<0.10	<0.003
13 July D	<0.072	<0.004	0.567	<0.065	0.092	<0.019	<0.10	<0.003

b.

	α-HCH	γ-HCH	PCB28	PCB52	PCB101	*p,p'*-DDE	PBDE47		PBDE99	
	g	g	g	g	g	g	g	p	g	p
3 July D	0.078	0.242	0.037	0.023	0.008	0.015	<0.38	n.d.	<0.30	n.d.
3-4 July N	0.055	0.194	0.024	0.016	0.009	0.012	<0.38	n.d.	<0.30	n.d.
4 July D	0.008	0.007	0.006	0.003	0.005	0.003	<0.38	n.d.	<0.30	n.d.
4-5 July N	n.d.	n.d.	n.d.	n.d.	n.d.	n.d.	n.d.	n.d.	n.d.	n.d.
5 July D	0.028	0.105	0.015	0.009	0.006	0.006	<0.38	n.d.	<0.30	n.d.
5-6 July N	n.d.	n.d.	n.d.	n.d.	n.d.	n.d.	n.d.	n.d.	n.d.	n.d.
6 July D	0.017	0.042	0.021	0.010	<0.012	<0.008	0.500	0.161	0.313	0.203
6-7 July N	0.053	0.123	0.021	0.012	0.003	<0.008	<0.38	0.110	0.214	0.166
7 July D	0.029	0.065	0.022	0.010	<0.012	<0.008	0.509	0.104	0.299	0.145
7-8 July N	0.039	0.115	0.023	0.014	0.006	0.006	0.317	0-108	0.161	0.140
8 July D	0.024	0.074	0.020	0.010	<0.012	<0.008	0.345	0.132	0.264	0.192
8-9 July N	0.055	0.189	0.032	0.024	0.011	0.007	0.251	0.113	0.209	0.174
9 July D	0.019	0.046	0.024	0.010	<0.012	0.005	0.203	0.114	0.137	0.147
9-10 July N	0.076	0.245	0.033	0.024	0.011	0.007	0.228	0.135	0.197	0.152
10 July D	0.042	0.154	0.022	0.014	0.005	0.004	<0.38	0.134	<0.30	0.159
10-11 July N	0.014	0.066	<0.015	0.005	<0.012	<0.008	<0.38	0.110	0.141	0.137
11 July D	0.027	0.066	0.030	0.013	<0.008	0.010	0.262	0.105	<0.30	0.134
11-12 July N	<0.015	0.057	0.008	0.005	<0.012	<0.008	<0.38	n.d.	0.249	n.d.

12 July D	<0.015	0.038	0.008	0.003	<0.012	<0.008	<0.38	n.d.	<0.30	n.d.
12-13 July N	<0.015	0.030	0.008	0.003	<0.012	<0.008	<0.38	n.d.	<0.30	n.d.
13 July D	0.042	0.145	0.016	0.013	<0.012	0.004	<0.38	n.d.	<0.30	n.d.

Table S4. Vertical concentration differences, $\Delta c_z = c_{z2}-c_{z1}$, of gaseous (a.) gaseous and particulate PAHs (ng m^{-3}), and (b.) gaseous OCPs (ng m^{-3}), PCBs (ng m^{-3}) and gaseous and particulate PBDEs (pg m^{-3}). Δz = 1.75 m. Upper limits: Insignificant values of concentration differences (<6 standard deviations of field blank concentrations). c_{z1} data from 6 July D until 10 July D based on 2 replica measurements (mean).

a.

	ACE		PHE		FLT		PYR	
	g	p	g	p	g	p	g	P
3 July D	<0.058	<0.007	7.35	<±0.129	-0.46	<±0.037	-0.15	n.d.
3-4 July N	<0.096	<0.007	5.55	<±0.129	-0.25	0.047	0.11	n.d.
4 July D	<0.058	<0.007	0.65	<±0.129	-0.24	<±0.037	-0.42	n.d.
4-5 July N	n.d.	n.d.	n.d.	n.d.	n.d.	n.d.	n.d.	n.d.
5 July D	<0.072	<0.007	0.53	<±0.129	-0.39	0.048	-0.13	n.d.
5-6 July N	n.d.	n.d.	n.d.	n.d.	n.d.	n.d.	n.d.	n.d.
6 July D	0.10	<±0.007	1.48	-0.248	<±0.076	-0.111	<±0.076	-0.041
6-7 July N	-0.024	<±0.007	<±0.37	<±0.129	0.18	<±0.037	<±0.076	-0.006
7 July D	-0.026	<±0.007	<±0.37	<±0.129	<±0.076	<±0.037	<±0.076	<±0.005
7-8 July N	<±0.013	<±0.007	0.62	<±0.129	0.37	<±0.037	0.14	<±0.005
8 July D	-0.019	<±0.007	0.76	<±0.129	0.41	<±0.037	0.16	<±0.005
8-9 July N	<±0.013	<±0.007	0.97	<±0.129	0.89	<±0.037	0.40	0.056
9 July D	n.d.	n.d.	n.d.	n.d.	n.d.	n.d.	n.d.	n.d.
9-10 July N	0.037	<±0.007	0.80	<±0.129	0.95	<±0.037	0.45	<±0.005
10 July D	n.d.	<±0.007	0.51	<±0.129	0.73	<±0.037	0.32	0.059
10-11 July N	n.d.	n.d.	n.d.	n.d.	n.d.	n.d.	n.d.	n.d.
11 July D	n.d.	n.d.	<±0.37	n.d.	0.15	n.d.	<±0.075	n.d.
11-12 July N	n.d.	n.d.	<±0.37	n.d.	0.12	n.d.	<±0.075	n.d.
12 July D	n.d.	n.d.	<±0.37	n.d.	<±0.076	n.d.	<±0.075	n.d.
12-13 July N	n.d.	n.d.	<±0.37	n.d.	0.44	n.d.	0.18	n.d.
13 July D	n.d.	n.d.	7.35	n.d.	-0.46	n.d.	-0.15	n.d.

b.

	α-HCH	*γ*-HCH	PCB28	PCB52	PCB101	*p,p'*-DDE	PBDE47		PBDE99	
	g	*g*	g	g	g	g	g	p	g	p
3 July D	0.675	0.890	0.155	0.120	0.044	<±0.008	n.d.	n.d.	n.d.	n.d.
3-4 July N	0.258	0.510	0.103	0.089	0.035	<±0.008	n.d.	n.d.	n.d.	n.d.
4 July D	0.187	0.483	0.080	0.052	0.016	<±0.008	n.d.	n.d.	n.d.	n.d.
4-5 July N	n.d.	n.d.	n.d.	n.d.	n.d.	n.d.	n.d.	n.d.	n.d.	n.d.
5 July D	0.147	0.313	0.060	0.035	0.011	<±0.008	n.d.	n.d.	n.d.	n.d.
5-6 July N	n.d.	n.d.	n.d.	n.d.	n.d.	n.d.	n.d.	n.d.	n.d.	n.d.
6 July D	0.078	0.189	0.029	0.012	n.d.	n.d.	-0.28	<±0.076	<±0.33	<±0.099
6-7 July N	-0.036	-0.057	<±0.016	<±0.007	n.d.	n.d.	n.d.	<±0.076	n.d.	<±0.099
7 July D	<±0.020	-0.041	<±0.016	<±0.007	n.d.	n.d.	n.d.	<±0.076	n.d.	<±0.099
7-8 July N	-0.025	-0.048	<±0.016	<±0.007	<±0.008	<±0.008	n.d.	<±0.076	n.d.	<±0.099
8 July D	<±0.020	-0.018	<±0.016	<±0.007	n.d.	n.d.	<±0.24	<±0.076	<±0.33	<±0.099
8-9 July N	-0.025	-0.082	<±0.016	-0.0089	<±0.008	<±0.008	n.d.	<±0.076	<±0.33	<±0.099
9 July D	<±0.020	0.037	<±0.016	<±0.007	n.d.	n.d.	n.d.	-0.114	n.d.	-0.147
9-10 July N	-0.048	-0.159	<±0.016	-0.011	<±0.008	<±0.008	n.d.	<±0.076	n.d.	<±0.099
10 July D	<±0.020	-0.052	<±0.016	<±0.007	<±0.008	0.0091	n.d.	<±0.076	n.d.	<±0.099
10-11 July N	n.d.	n.d.	n.d.	n.d.	n.d.	n.d.	n.d.	n.d.	n.d.	n.d.
11 July D	<±0.020	0.088	<±0.016	<±0.007	n.d.	<±0.008	n.d.	-0.105	n.d.	-0.134
11-12 July N	n.d.	-0.030	<±0.016	<±0.007	n.d.	n.d.	n.d.	n.d.	n.d.	n.d.
12 July D	n.d.	<±0.019	<±0.016	<±0.007	n.d.	n.d.	n.d.	n.d.	n.d.	n.d.
12-13 July N	n.d.	<±0.019	<±0.016	<±0.007	n.d.	n.d.	n.d.	n.d.	n.d.	n.d.
13 July D	<±0.020	-0.073	0.017	<±0.007	n.d.	<±0.008	n.d.	n.d.	n.d.	n.d.

Table S5. Vertical fluxes $F_c = -v_{tr} \Delta c_z$ of gaseous (a.) PAHs (µg m^{-2} d^{-1}), and (b.) OCPs (µg m^{-2} d^{-1}), PCBs (µg m^{-2} d^{-1}) and PBDEs (ng m^{-2} d^{-1}). Positive = upward, negative = downward. Empty fields = no data. Insignificant data (<6 standard deviations of field blank concentrations) given as upper limits.

a.

	ACE	PHE	FLT	PYR
3 July D		-28.46	1.80	0.59
3-4 July N				
4 July D		-2.41	0.94	1.56
4-5 July N				
5 July D		-1.33	0.97	0.33
5-6 July N				
6 July D	-0.34	-4.84	<±0.25	<±0.24
6-7 July N				
7 July D	0.16	<±2.26	<±0.47	<±0.46
7-8 July N				
8 July D	0.12	-4.72	-2.57	-1.02
8-9 July N				
9 July D				
9-10 July N				
10 July D		-2.06	-2.97	-1.32
10-11 July N				
11 July D				
11-12 July N		<±1.44	-0.59	<±0.29
12 July D		<±1.57	-0.51	<±0.32
12-13 July N		<±1.03	<±0.21	<±0.21
13 July D		<±0.89	-1.06	-0.44

b.

	α-HCH	γ-HCH	PCB28	PCB52	PCB101	*p,p'*-DDE	PBDE47	PBDE99
3 July D	-2.61	-3.45	-0.60	-0.47	-0.17	<±0.03		
3-4 July N								
4 July D	-0.69	-1.79	-0.30	-0.19	-0.06	<±0.03		
4-5 July N								
5 July D	-0.37	-0.78	-0.15	-0.09	-0.03	<±0.02		
5-6 July N								
6 July D	-0.26	-0.62	-0.09	-0.04			0.91	<±1.09
6-7 July N								
7 July D	<±0.12	0.25	<±0.10	<±0.04				
7-8 July N								
8 July D	<±0.12	0.11	<±0.10	<±0.04			<±1.47	<±2.08
8-9 July N								
9 July D	<±0.13	0.23	<±0.10	<±0.04				
9-10 July N								
10 July D	<±0.08	-0.21	<±0.06	<±0.03	<±0.03	0.04		
10-11 July N								
11 July D	<±0.06	0.26	<±0.05	<±0.02		<±0.02		
11-12 July N		-0.12	<±0.06	<±0.03				
12 July D		<±0.08	<±0.07	<±0.03				
12-13 July N		<±0.05	<±0.04	<±0.02				
13 July D	<±0.05	0.18	-0.04	<±0.02		<±0.02		

S2.4 Seawater concentration data

Table S6. Concentrations in surface seawater at two localities west of Selles Beach and arithmetic mean (pg L^{-1}).

	c_w at locality 1	c_w at locality 2	mean c_w
FLT	21.2	15.3	18.2
PYR	6.3	2.6	4.4
PCB 28	4.73	4.58	4.65
PCB 52	0.53	0.54	0.54
PCB 101	0.84	0.85	0.84
p,p'-DDE	0.75	0.93	0.84
BDE 47	0.12	0.18	0.15
BDE 99	0.039	0.037	0.038

S2.5 Model predicted concentrations and air-sea exchange flux

During the period 6−10 July, Crete was under influence of a constant northerly flow during day and night without change of air mass (see above, S2.1).

Many pollutants showed pronounced night-time maxima: c_{day}/c_{night} = 0.3− 0.5 for HCH isomers, 0.6−0.7 for ACE, PHE, DDE and PCB52. For other species this was less pronounced or no day/night trend was observed (c_{day}/c_{night} = 0.8–0.9 for PCB28, FLT, PYR, 1.1−1.3 for PBDEs) (Fig. 1).

During on-shore advection many contaminants' concentrations were influenced by BL depth, as indicated by anti-correlation with PAHs and OCPs (except DDE; r = -0.76 − -0.37 i.e., significant for α-HCH on the $p < 0.05$ confidence level, t-test). BL depth was not correlated with PCBs' and DDE concentrations ($|r| < 0.45$). These findings indicate sea surface sources.

Using the 2-box fugacity model (above, S1.4), air–sea mass exchange fluxes, F_{em}, in the range -1000 − +10 ng m^{-2} h^{-1} (positive defined upward) and atmospheric concentrations fed by F_{em} only in the range 0.01−2.2 ng m^{-3} are simulated (Table S7).

Table S7. Predicted concentrations in the marine atmospheric BL and surface seawater (mean (min-max), ng m^{-3}) and air–sea mass exchange fluxes, F_{em} (mean (min-max), ng m^{-2} h^{-1})

	c_a (ng m^{-3})	c_w (ng m^{-3})	F_{em} (ng m^{-2} d^{-1})
FLT	0.51 (0.13–2.27)	20.6 (18.2–22.0)	-3.20 (-13.6–0.00)
PYR	0.13 (0.01–1.13)	5.41 (4.44–5.60)	-0.96 (-9.32–0.08)
PCB28	0.037 (0.011–0.11)	4.60 (4.55–4.65)	0.061 (-0.009–0.14)
PCB52	0.016 (0.005–0.049)	0.54 (0.54–0.54)	-0.007 (-0.041–0.007)
BDE47	0.45 (0.12–2.04)	4.00 (0.15–6.41)	-5.22 (-20.0–0.00)
BDE99	0.25 (0.051–1.27)	3.34 (0.49–4.89)	-3.69 (-15.3–0.00)

Fig. S4. Predicted vertical flux, F_c (red upward and blue downward, ng m^{-2} d^{-1}), of selected pollutants i.e. (a) PYR, (b) PCB52, (c) BDE99 during 6-10 July 2012 (see also Fig. 2).

a.

b.

c.

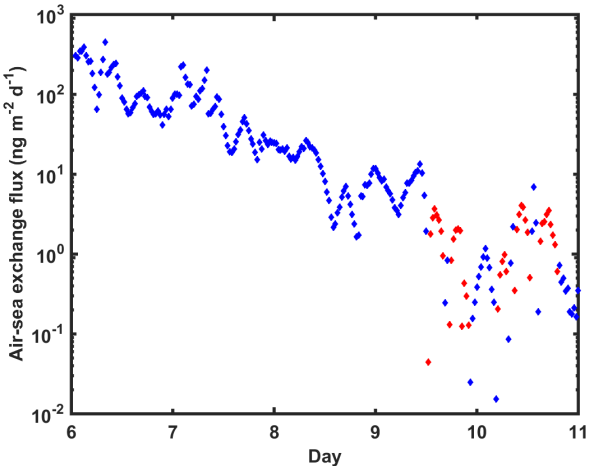
Air-sea exchange flux (ng m-2 d-1)
Day

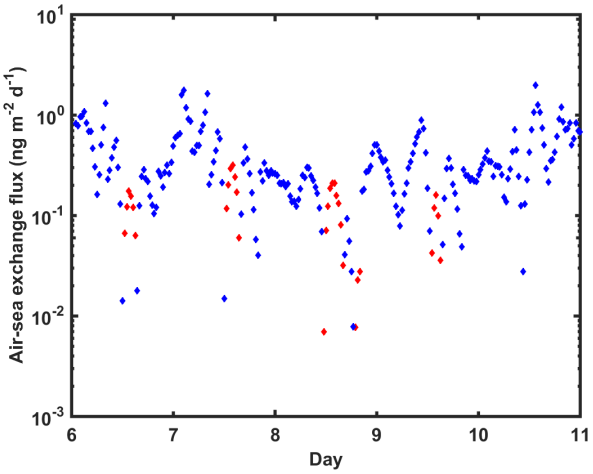
Air-sea exchange flux (ng m-2 d-1)
Day

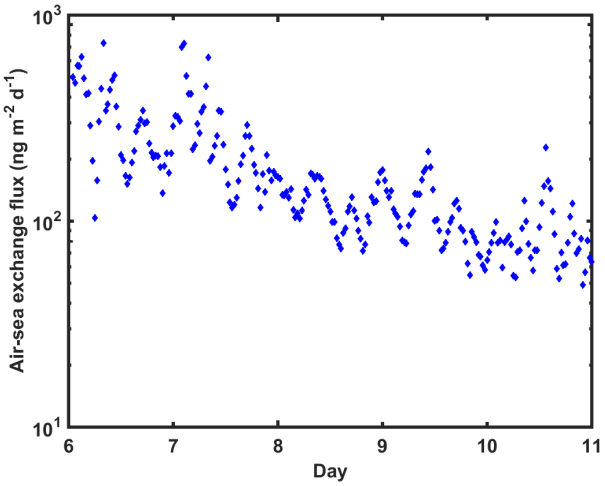
Air-sea exchange flux (ng m-2 d-1)
Day

References

Anderson, P.N., Hites, R.A., 1996. Hydroxyl radical reactions: The major pathway for polychlorinated biphenyls from the atmosphere. Environ. Sci. Technol. 30, 1756-1763.

Bamford, H.A., Poster, D.L., Baker, J.E., 1999. Temperature dependence of Henry's law constants of thirteen polycyclic aromatic hydrocarbons between 4°C and 31°C, Environ. Toxicol. Chem. 18, 1905-1912.

Beyer, A., Mackay, D., Matthies, M., Wania, F., Webster, E., 2000. Assessing long-range transport potential of persistent organic pollutants, Environ. Sci. Technol. 34, 699-703.

Cetin, B., Odabasi, M., 2005. Measurement of Henry's law constants of seven polybrominated diphenylethers (PBDE) congeners as a function of temperature. Atmos. Environ. 39, 5273-5280

Cetin, B., Özer, S., Sofuoglu, A., Odabasi, M., 2006. Determination of Henry's law constants of organochlorine pesticides in deionized and saline water as a function of temperature. Atmos. Environ. 40, 4538-4546.

d'Ortenzio, F., Iudicone, D., de Boyer Montegut, C., Testor, C., Antoine, D., Marullo, S., Santoleri, R., Madec, G., 2005. Seasonal variability of the mixed layer depth in the Mediterranean Sea as derived from in situ profiles, Geophys. Res. Lett. 32, L12605.

Dyer AJ, 1974. A review of flux-profile relationships. Boundary-Layer Meteor. 7, 363-372

EU, 1996. Technical guidance document in support of the commissions directive 5 93/67/EEC on risk assessment for the notified substances and the commission regulation (EC) 1488/94 on risk assessment for existing substances.

Foken, T., 2008. Micrometeorology, Springer, Heidelberg, 308 pp.

Franklin, J., Atkinson, R., Howard, P.H., Orlando, J.J., Seigneur, C., Wallington, T.J., Zetzsch, C., 2000. Quantitative determination of persistence in air, in: Evaluation of Persistence and Long-Range Transport of Organic Chemicals in the Environment (Klecka, G.M., et al., eds.), SETAC Press, Pensacola, USA, pp. 7–62.

Hayward, S.J., Lei, Y.D., Wania, F., 2006. Comparative evaluation of three HPLC-based K_{ow} estimation methods for highly hydrophobic organic compounds: PBDEs and HBCD, Environ. Toxicol. Chem. 25, 2018-2027.

Hicks, B.B., Baldocchi, D.D., Meyers, T.P., Hosker, R.P., Matt, D.R., 1987. A preliminary multiple resistance routine for deriving dry deposition velocities from measured quantities, Water Air Soil Poll. 36, 311–330.

Jantunen, L.M., Bidleman, T.F., 2006. Henry's law constants for hexachlorobenzene, *p,p'*-DDE and components of technical chlordane and estimates of gas-exchange for Lake Ontario, Chemosphere 62, 1689-1696.

Jonker, M.T.O., Muijs, B., 2010. Using solid phase micro extraction to determine salting-out (Setschenow) constants for hydrophobic organic chemicals. Chemosphere 80, 223–227.

Karickhoff, S.W., 1981. Semi-empirical estimation of sorption of hydrophobic pollutants on natural sediments and soils. Chemosphere 10, 833-849.

Keyte, I.J., Harrison, R.M., Lammel, G., 2013. Chemical reactivity and long-range transport potential of polycyclic aromatic hydrocarbons – a review, Chem. Soc. Rev. 42, 9333-9391

Kuhn, U., Andreae, M.O., Ammann, C., Araujo, A. C., Brancaleoni, E., Ciccioli, P., Dindorf, T., Frattoni, M., Gatti, L. V., Ganzeveld, L., Kruijt, B., Lelieveld, J., Lloyd, J., Meixner, F. X., Nobre, A. D., Pöschl, U., Spirig, C., Stefani, P., Thielmann, A., Valentini, R., Kesselmeier, J., 2007. Isoprene and monoterpene fluxes from Central Amazonian rainforest inferred from tower-based and airborne measurements, and implications on the atmospheric chemistry and the local carbon budget, Atmos. Chem. Phys. 7, 2855–2879.

Li, N., Wania, F., Lei, Y.D., Daly, G.L., 2003. A comprehensive and critical compilation, evaluation, and selection of physical-chemical property data for selected polychlorinated biphenyls. J. Phys. Chem. Ref. Data, 32, 1545–1590.

Lohmann, R., Klánová, J., Kukučka, P., Yonis, S., Bollinger, K., 2012. PCBs and OCPs on a east to west transect: The importance of major currents and net volatilization for PCBs in the Atlantic Ocean, Environ. Sci. Technol. 46, 10471-10479.

Monin, A.S., Obukhov, A.M., 1954. Osnovnye zakonommernosti turbulentnogo peremesivanija v prizemnom sloe atmosfery, Trudy Geofiz. Inst. AN SSSR, 24 (151), 163–187.

Mulder, M.D., Heil, A., Kukučka, P., Klánová, J., Kuta, J., Prokeš, R., Sprovieri, F., Lammel, G., 2014. Air-sea exchange and gas-particle partitioning of polycyclic aromatic hydrocarbons in the Mediterranean. Atmos. Chem. Phys. 14, 8905–8915.

Obukhov, A.M., 1948. Turbulentnost' v temperaturnoj - neodnorodnoj atmosphere (Turbulence in an atmosphere with a non-uniform temperature), Trudy Inst. Theor. Geofiz. AN SSSR 1, 95-115.

Paulson, C.A., 1970. The mathematical representation of wind speed and temperature profiles in the unstable atmospheric surface layer. J. Appl. Meteor. 9, 857-861.

Pujo-Pay, M., Conan, P., Oriol, L., Cornet-Barthaux, V., Falco, C., Ghiglione, J.F., Goyet, C., Moutin, T., Prieur, L., 2011. Integrated survey of elemental stoichiometry (C, N, P) from the western to eastern Mediterranean Sea, Biogeosci. 8, 883-899.

Raff, J.D., Hites, R.A., 2007. Deposition vs. photochemical removal of PBDEs from Lake Superior air, Environ. Sci. Technol. 41, 6725-6731.

Rowe, A. A., Totten, L. A., Xie, M., Fikslin, T. J., Eisenreich, S. J., 2007. Air-water exchange of polychlorinated biphenyls in the Delaware river. Environ. Sci. Technol. 41, 1152–1158.

Schwarzenbach, R.P., Gschwend, P.M., Imboden, D.M., 2003: Environmental Organic Chemistry, 2nd ed., Wiley, Hoboken, USA.

Spivakovsky, C.M., Logan, J.A., Montzka, S.A., Balkanski, Y.J., Foreman-Fowler, M., Jones, D.B.A., Horowitz, L.W., Fusco, A.C., Brenninkmeijer, C.A.M., Prather, M.J., Wofsy, S.C., McElroy, M.B., 2000. Three-dimensional climatological distribution of tropospheric OH: update and evaluation. J. Geophys. Res. 105, 8931–8980.

Tittlemier, S.A., Halldorson, T., Stern, G.A., Tomy, G., 2002. Vapor pressures, aqueous solubilities, and Henry law constants of some brominated flame retardants. Environ. Toxicol. Chem. 21, 1804-1810.

USEPA, 2009. EPI Suite v4.0, Exposure assessment tools and models, US Environmental Protection Agency. http://www.epa.gov/opt/exposure/pubs/episuitedl.

Valavanis, V.D., Georgakarakos, S., Kapantagakis, A., Palialaxis, A., Katara, I., 2004. A GIS environmental modelling aproach to essential fish hapital designation. Ecol. Model. 178, 417-427.

Wania, F., Daly, G., 2002. Estimating the contribution of degradation in air and deposition to the deep sea to the global loss of PCBs. Atmos. Environ. 36, 5581-5593.

Zhong G., Xie Z., Möller A., Halsall C., Caba A., Sturm R., Tang J., Zhang G., Ebinghaus R., 2012. Currently used pesticides, hexachlorobenzene and hexachlorocyclohexanes in the air and seawater of the German Bight (North Sea). Environ. Chem. 9, 405-414.